Original Article

MOLECULAR METABOLISM

Indoleamine 2,3-dioxygenase mediates the therapeutic effects of adipose-derived stromal/stem cells in experimental periodontitis by modulating macrophages through the kynurenine-AhR-NRF2 pathway

Hanyue Li [1,2,3], Yu Yuan [1,2,3], Hongying Chen [1,2,3], Hongwei Dai [1,2,3,**], Jie Li [1,2,3,*]

ABSTRACT

Objectives: Mesenchymal stromal/stem cell (MSC)-based therapy has become a promising approach to periodontal tissue repair. Adipose-derived stromal/stem cells (ASCs), compared with other dental or non-dental MSCs, serve as promising candidates for MSC therapy due to non-invasive acquisition and abundant sources. This study aimed to explore the effects of ASC therapy in experimental periodontitis and the underlying mechanism.

Methods: Micro-CT was performed to evaluate the alveolar bone parameters following local injection of ASCs. Immunohistochemistry and immunofluorescence were employed to detect the expression of IL-1β, osteocalcin (OCN), nuclear factor (erythroid-derived 2)-like 2 (NRF2), and surface markers of macrophage polarization. Afterward, multiple reaction monitoring (MRM)-based targeted tryptophan metabolomic analysis was used to examine the ASC metabolites. Chromatin immunoprecipitation (ChIP)-qPCR assay was performed to investigate the direct binding of aryl hydrocarbon receptor (AhR) and NRF2.

Results: Alveolar bone loss was reduced, and the ratio of $iNOS^{+}/CD206^{+}$ macrophages was significantly decreased after ASC injection in the rat models of periodontitis. ASCs promoted NRF2 expression and activation in macrophages, while NRF2 silencing in macrophages blocked the regulation of ASCs on macrophages. Furthermore, the expression of indoleamine 2,3-dioxygenase (IDO) of ASCs in the inflammatory condition was high. The inhibitor of IDO, 1-methyltryptophan (1-MT), impaired the therapeutic effects of ASCs in experimental periodontitis and regulation of macrophage polarization. Mechanistically, kynurenine (Kyn), a metabolite of ASCs catalyzed by IDO, activated AhR and enhanced its binding to the promoter of NRF2, which stimulated M2 macrophage polarization.

Conclusions: These findings suggested that ASCs can alleviate ligature-induced periodontitis through modulating macrophage polarization by the IDO-dependent Kyn-AhR-NRF2 pathway, uncovering a novel mechanism and providing a scientific basis for ASC-based therapy in experimental periodontitis.

Keywords Adipose-derived stromal/stem cells (ASCs); Experimental periodontitis; Macrophages; Indoleamine 2,3-dioxygenase (IDO); Therapy

1. INTRODUCTION

Periodontitis is a common oral disease affecting more than half of adults. It primarily leads to the destruction of periodontal tissues (periodontal ligament, alveolar bone, and gingiva), eventually resulting in tooth loosening and loss [1].

To date, the treatment of periodontitis remains challenging. Recently, mesenchymal stromal/stem cell (MSC)-based therapy has become a promising approach for periodontal tissue repair. In pre-clinical research, MSC delivery, including dental MSCs (such as periodontal ligament stem cells (PDLSCs), dental pulp-derived stem cells, dental follicle stem cells, etc.) and non-dental MSCs, has been demonstrated to

[1]College of Stomatology, Chongqing Medical University, Chongqing, 401147, China [2]Chongqing Key Laboratory of Oral Diseases and Biomedical Sciences, Chongqing Medical University, Chongqing, 401147, China [3]Chongqing Municipal Key Laboratory of Oral Biomedical Engineering of Higher Education, Chongqing Medical University, Chongqing, 401147, China

*Corresponding author. College of Stomatology, Chongqing Medical University, 426# Songshibei Road, Yubei District, Chongqing, 401147, PR China. Fax: +86 23 8886 0222. E-mail: jieli@hospital.cqmu.edu.cn (J. Li).

**Corresponding author. College of Stomatology, Chongqing Medical University, 426# Songshibei Road, Yubei District, Chongqing, 401147, PR China. Fax: +86 23 8886 0222. E-mail: dai64@hospital.cqmu.edu.cn (H. Dai).

Received July 18, 2022 • Revision received September 9, 2022 • Accepted October 14, 2022 • Available online 18 October 2022

https://doi.org/10.1016/j.molmet.2022.101617

Abbreviations

ASCs	adipose-derived stromal/stem cells
AhR	aryl hydrocarbon receptor
ALI	acute liver injury
ALP	alkaline phosphatase
ARS	alizarin red S
BV/TV	Bone Volume/Total Volume
ChIP	chromatin immunoprecipitation
CEJ-ABC	cementoenamel junction and alveolar bone crest
ELISA	enzyme-linked immunosorbent assay
3-Haa	3-hydroxyanthranilic acid
IDO	indoleamine 2,3-dioxygenase
Kyn	kynurenine
Ka	kynurenic acid
Pic	picolinic acid
MSC	mesenchymal stromal/stem cells
MRM	multiple reaction monitoring
1-MT	1-methyl-D-tryptophan
NRF2	nuclear factor (erythroid-derived 2)-like 2
PDLSCs	periodontal ligament stem cells
PBS	phosphate buffered saline
PMA	phorbol-12-myristate-13-acetate
Quin	quinolinic acid
ROS	reactive oxygen species
Trp	tryptophan
Tb. Th	Trabecular Thickness
Tb. Sp	Trabecular Separation

yield reliable and effective therapeutic outcomes in periodontitis models and clinical trials are either underway or are in preparation [2–4].

Adipose-derived stromal/stem cells (ASCs) are considered promising candidates for MSC-based therapy owing to their convenience for acquisition, abundant quantities, and robust immune-regulatory abilities compared with other MSCs [5,6]. Although ASCs and PDLSCs display similar properties of MSCs, PDLSCs exhibit more potent cementoblastic/osteoblastic differentiation capacities while ASCs show stronger immunomodulatory properties [7,8]. Besides, the quantities of PDLSCs are limited compared with ASCs, which are abundant in adipose tissues and can maintain stemness after several passages. Earlier studies have validated that the transplantation of ASCs with biologic materials or platelet-rich plasma in alveolar bone defects promoted periodontal tissue regeneration [9,10], indicating the potential therapeutic effects of ASCs in periodontitis. However, the cellular mechanism is unclear. In addition to multi-differentiation potential, ASCs also possess potent immunomodulatory capacities, including regulating macrophage polarization, which creates a favorable milieu and empowers the neighboring cells to repair [11,12]. Previous research has corroborated that ASCs mitigated various inflammatory and immune diseases by skewing macrophages toward anti-inflammatory M2 phenotypes [13,14]. Given that macrophages serve as the first line of defense in immunity, of which the polarization determines the inflammatory progression and healing process in periodontitis [15], the modulation of macrophages by ASCs might contribute to periodontal tissue repair.

Recently, the immunomodulatory capacities of MSCs, including macrophage regulation, have been reported to be associated with metabolism and their therapeutic effects [16–19]. Indoleamine 2,3-dioxygenase (IDO) is not only regarded as a core immunoregulator but also an initial rate-limiting enzyme of tryptophan (Trp) metabolism, catalyzing Trp to kynurenine (Kyn) and further breaking down into other intermediates [20], which played critical roles in macrophage polarization [21–23]. The ratio of Trp/Kyn indicates the activity of IDO. A recent study reported that the IDO-mediated metabolite kynurenic acid (Ka) derived from MSCs exerted immunosuppressive effects on T cells in acute liver injury (ALI) mice models [17]. However, whether Trp metabolism is implicated in ASC-mediated modulation of macrophages is unclear.

In this study, we investigated the therapeutic effects of ASCs in ligature-induced periodontitis and explored the underlying mechanism. Our results demonstrated that ASCs alleviated alveolar bone loss in periodontitis by regulating macrophages through nuclear factor (erythroid-derived 2)-like 2 (NRF2). Further mechanistic studies revealed that IDO-mediated Kyn activated AhR and enhanced binding to the promoter of NRF2 in macrophages.

2. MATERIALS AND METHODS

2.1. Isolation and identification of human ASCs and PDLSCs

All procedures were carried out in accordance with the ethical standards of the Ethics Committee of the College of Stomatology, Chongqing Medical University (approval no. CQHS-REC-2021 (LSNo. 43); CQHS-REC-2022 (LSNo. 006)). ASCs were isolated as we previously described [24]. Human adipose tissue from six healthy donors (aged 20–40 years) was obtained by liposuction procedures under anesthesia following informed consent. Briefly, the clean adipose tissue samples were digested with an equal volume of 0.1% type I collagenase (Sigma–Aldrich, MO, USA), shaking at a speed of 200 rpm and 37 °C for 60 min. After digestion, samples were spun and the top layer of oil and fat and the underlying layer of collagenase solution were carefully removed. After washed three times by phosphate buffer saline (PBS), cells were resuspended by culture medium (α-minimum essential medium (α-MEM, HyClone, UT, USA) supplemented with 10% fetal bovine serum (FBS, Gibco, Australia) and 1% penicillin/streptomycin.

PDLSCs were isolated from premolars extracted from donors (aged 12–25 years) who were undergoing orthodontic treatment. The extracted teeth were washed three times by sterile PBS. Next, the PDL tissues were obtained from the middle third of the root surface and digested in 3 mg/mL type I collagenase for 30 min at 37 °C. Tissues were seeded into cell culture flasks with α-MEM supplemented with 10% FBS and 1% penicillin/streptomycin.

To identify ASC and PDLSC phenotypes, flow cytometry was performed to assess the surface markers. Human CD31, CD34, CD45, CD90, CD105 and CD73 (BD Biosciences, CA, USA) were detected. To evaluate the multi-differentiation potential, osteogenic differentiation medium was used to culture cells and cells were stained with 1% alizarin red solution (Sigma–Aldrich) after 21 days. Adipogenic differentiation medium was used to culture cells and after 14 days cells were stained with oil red O (Solarbio, Beijing, China).

2.2. U937 cell culture and macrophage induction

Human monocyte cell line U937 cells were purchased from Procell company (Wuhan, China), cultured in RPMI 1640 containing 10% FBS (Biological Industries, Israel) and 1% antibiotics at 37 °C in 5% CO_2. U937 cells were induced into macrophages by using 100 ng/mL

phorbol-12-myristate-13-acetate (PMA, Sigma—Aldrich) for 48 h until cells adhered to the culture plate.

2.3. Coculture system

U937 macrophages (5×10^5) were plated in the six well plate, while ASCs (5×10^5) were loaded into the upper chamber of the transwell insert (0.4 μm, Corning, NY, USA). 1 μg/mL lipopolysaccharide (LPS) (Sigma—Aldrich) was added in the coculture system for 24 h. Under certain conditions, ASCs were pretreated with a specific inhibitor of IDO, 500 μM 1-methyl-tryptophan (1-MT; Sigma—Aldrich) for 24 h and then were cocultured with macrophages for another 24 h with LPS stimulation. The culture media and cell lysates were collected.

2.4. Ligature-induced periodontitis rat models

4—6 weeks male Sprague Dawley (SD) rats were purchased from Chengdu Dossy Experimental Animals Co., Ltd (Chengdu, China). Animal experiments were approved by Ethics Committee of College of Stomatology, Chongqing Medical University (approval No. CQHS-REC-2021 (LSNo.43) and CQHS-REC-2022 (LSNo.006)). All rats were housed for at least 1 week before the experiments under a 12 h light/dark cycle at 23 ± 2 °C.

To induce experimental periodontitis, a 3-0 silk ligature was chosen to place around the bimaxillary second molar after rats were anesthetized with isoflurane inhalation. The ligatures were examined daily until 21 days of induction. The ligatures were removed and ASCs (1×10^6 suspended in 20 μL of PBS) or 1-MT-pretreated ASCs (1×10^6 suspended in 20 μL of PBS) were injected into the palatal side of the maxillary second molar at 1, 3, 9, 18 days. The contralateral sides of each rat were injected with equal PBS. Rats were sacrificed at 0, 7, 14, and 21 days with 6 rats at each time point.

2.5. Micro-computed tomography (Micro-CT)

The rat maxillae were scanned by Micro-CT (VivaCT 40; SCANCO Medical AG, Switzerland) using the settings of 70 kVp, 112 μA. Three-dimensional reconstructions were performed.

All samples were scanned with a sickness of 15 μm per slice. The cementoenamel junction and alveolar bone crest (CEJ-ABC) distance of the maxillary second molar were measured to evaluate the bone loss of the each rat. Bone parameters (Bone Volume/Total Volume (BV/TV), Trabecular Thickness (Tb. Th), Trabecular Separation (Tb. Sp)) were measured around the second molar. The region of the interest was the root furcation of the maxillary second molar including a 30-slice volume set at a threshold of 220 for analysis.

2.6. Immunohistochemical staining

The maxillae were fixed with 4% paraformaldehyde for 24 h and decalcified in 10% ethylenediaminetetraacetic acid (EDTA) disodium salt dehydrate for at least 2—3 months. Then samples were gradient dehydrated and embedded in paraffin. 5 μm sagittal sections were made, which were paralleled to the long axis of the second molar.

Heat-mediated antigen retrieval was performed using sodium citrate buffer. The sections were incubated with primary antibodies against IL-1β (1:100, A1112, Abclonal, Wuhan, China), osteocalcin (OCN) (1:50, 23418-1-AP, Proteintech, Wuhan, China), NRF2 (1:100, 16396-1-AP, Proteintech) overnight at 4 °C. HRP-conjugated secondary (ZSJQ-BIO, Beijing, China) was used to incubate for 30 min at room temperature, followed by diaminobenzidine (DAB) staining. Sections were scanned using SlideView VS200 (Olympus, Japan) and viewed by OlyVIA software (Olympus, Japan).

Three sections were chosen from each group. The positively stained area in the field was identified and quantified as mean density using the same value of color threshold (Image-Pro Plus).

2.7. Immunofluorescence assay

For tissues, the sections were incubated with a mouse anti-CD206 monoclonal antibody (1:100, 60143-1-Ig, Proteintech), a rabbit anti-NRF2 monoclonal antibody (1:100, A0674, Abclonal), a rabbit anti-inducible nitric oxide synthase (iNOS) polyclonal antibody (1:100, 18985-1-AP, Proteintech) overnight at 4 °C. After that, the sections were incubated with donkey anti-mouse IgG Alexa Flour 555 (1:200, Beyotime, Shanghai, China), or goat anti-rat IgG coralite 488 (1:100, Proteintech) for 30 min at room temperature. Nuclei were stained with DAPI (Beyotime).

For cells, anti-IL-1β antibody (1:100, A1112, Abclonal), anti-iNOS polyclonal antibody (1:100, 18985-1-AP, Proteintech), anti-CD206 monoclonal antibody (1:200, ET1702-4, Huabio, Hangzhou, China), anti-CD163 monoclonal antibody (1:100, ER1804-03, Huabio), anti-AhR monoclonal antibody (1:100, ab190797, Abcam, Cambridge, UK) and anti-NRF2 monoclonal antibody (1:100, A0674, Abclonal) were used.

Microscopic images were observed and taken with a fluorescent microscope (Olympus, Tokyo, Japan) and were analyzed by Image J software.

2.8. Osteogenic induction of PDLSCs

Conditioned medium (CM) of the cocultured cells was harvested (Figure 2E) and mixed (1:1) with α-MEM culture medium (containing 10% FBS and 1% penicillin/streptomycin) supplemented with the osteogenic ingredients (dexamethasone (0.1 μM), ascorbic acid (50 μg/mL) and β-glycerophosphate (10 mM) (Sigma—Aldrich)). The above medium was used to incubate PDLSCs and changed every 2 days. After 7 days, quantitative real-time polymerase chain reaction (RT-qPCR) and western blotting were performed.

2.9. Alkaline phosphatase (ALP) staining

After 7 days of induction, PDLSCs were fixed in 4% paraformaldehyde for 15 min followed by PBS washed twice. BCIP/NBT Alkaline Phosphatase Color Development Kit (Beyotime) was used to perform ALP staining according to the manufacturer's protocols.

2.10. Alizarin red S (ARS) staining

After 21 days of induction, PDLSCs were fixed in 4% paraformaldehyde for 15 min followed by PBS washed twice. 1% ARS (Sigma—Aldrich) was applied to examine the mineralized nodules.

2.11. Enzyme-linked immunosorbent assay (ELISA)

The CM of the indicated cells was collected to measure the concentration of tumor necrosis factor-alpha (TNF-α), IL-1β by ELISA (Novus, CO, USA) according to the product manual. The optical density (OD) was measured at a wavelength of 450 nm. The duplicate readings were averaged for each group. After subtracting the average zero standard optical density, a standard curve was created to calculate the concentration in each group.

2.12. RT-qPCR

Total RNA was isolated from macrophages, PDLSCs or ASCs with RNAiso Plus (Takara Biomedical Technology, Beijing, China) according to the manufacturer's manual. cDNA was synthesized by TaKaRa Prime-Script RT Reagent Kit (Takara Biomedical Technology, Beijing, China). qPCR was performed by a quantitative PCR System (Bio-Rad,

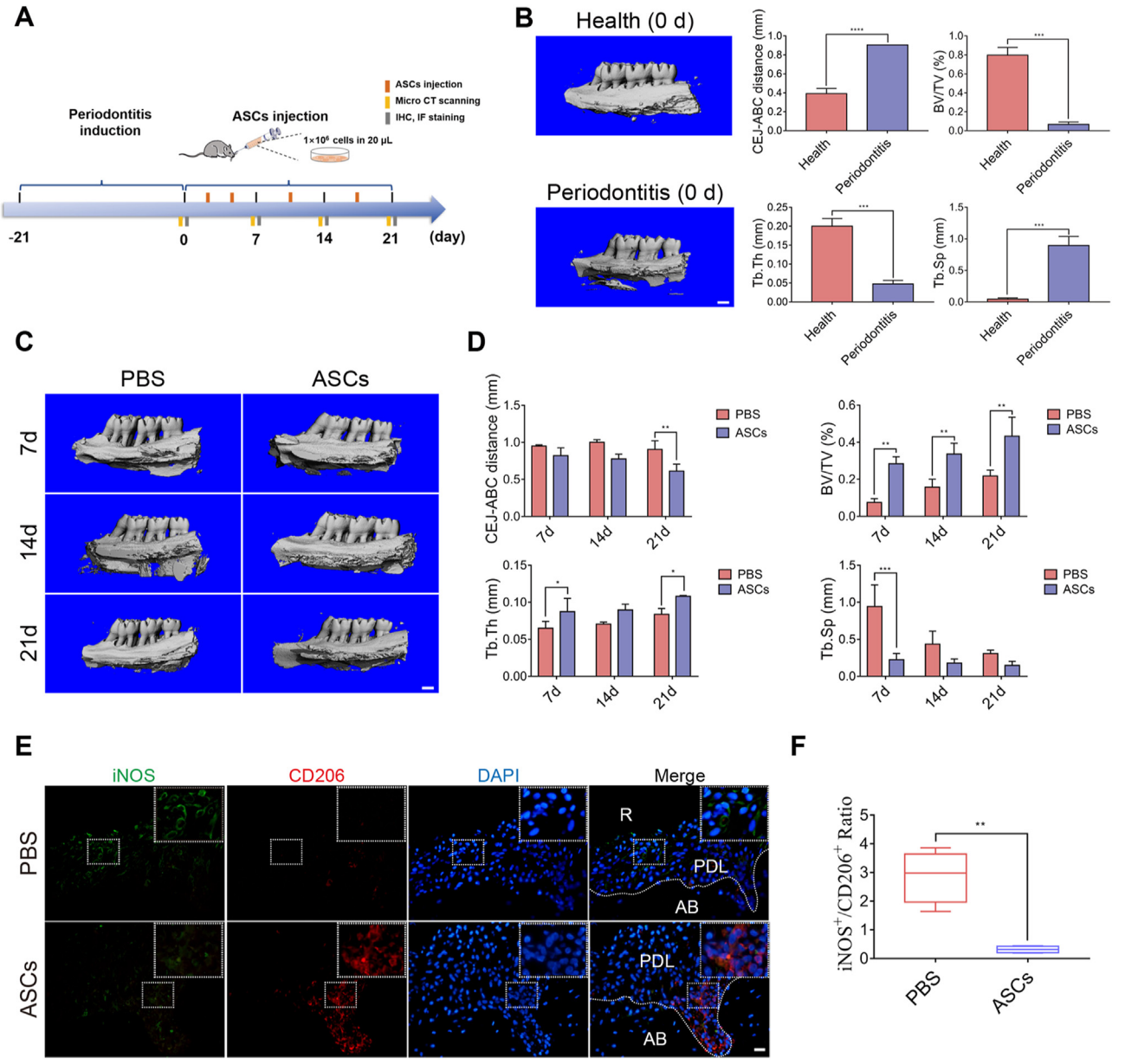

Figure 1: ASC therapeutic effects on experimental periodontitis in rats. (A) The schematic diagram showed the induction of the experimental rat model of periodontitis for 21 days and ASC injection after the removal of ligatures. (B) Micro-CT imaging and bone parameters (CEJ-ABC distance, BV/TV, Tb. Th, and Tb. Sp) between healthy and experimental rats of periodontitis. Scale bar, 1 mm. (C) Micro-CT imaging displayed the alveolar bone of PBS-injected and ASC-injected rats on day 7, day 14, and day 21 Scale bar, 1 mm. (D) The CEJ-ABC distance and bone parameters (BV/TV, Tb. Th, and Tb. Sp) between the PBS-injected and ASC-injected rats. (E) Representative immunofluorescence staining of M1 phenotype macrophages ($iNOS^+$; Green) and M2 macrophages ($CD206^+$; Red) in sagittal sections of maxillary molars in PBS-injected and ASC-injected rats. Scale bar, 20 μm. (F) The calculated ratio of $iNOS^+/CD206^+$ macrophages in PBS-injected and ASC-injected groups. CEJ-ABC, cementoenamel junction and alveolar bone crest. All data were expressed as mean ± SD; $^*P < 0.05$, $^{**}P < 0.01$, $^{***}P < 0.001$.

Hercules, CA, USA) using TB Green Premix Ex Taq II (Takara Biomedical Technology, Beijing, China). The primer sequences of the target genes are listed in Supplementary Table 1.

2.13. Nuclear protein extraction

Nuclear protein extracts were prepared by the nuclear and cytoplasmic extraction kit (Beyotime) according to the product manual.

2.14. Western blotting

The total proteins were extracted from cells by RIPA lysis buffer (Beyotime) with phenylmethanesulfonyl fluoride (PMSF; Beyotime) and then separated by sodium dodecyl sulfate-polyacrylamide gel electrophoresis (SDS-PAGE; Beyotime) transferring to polyvinylidene difluoride membranes (PVDF; Millipore, MA, USA). Primary antibodies against type I collagen (COL1) (1:1000, Bioss, Beijing, China), runt-

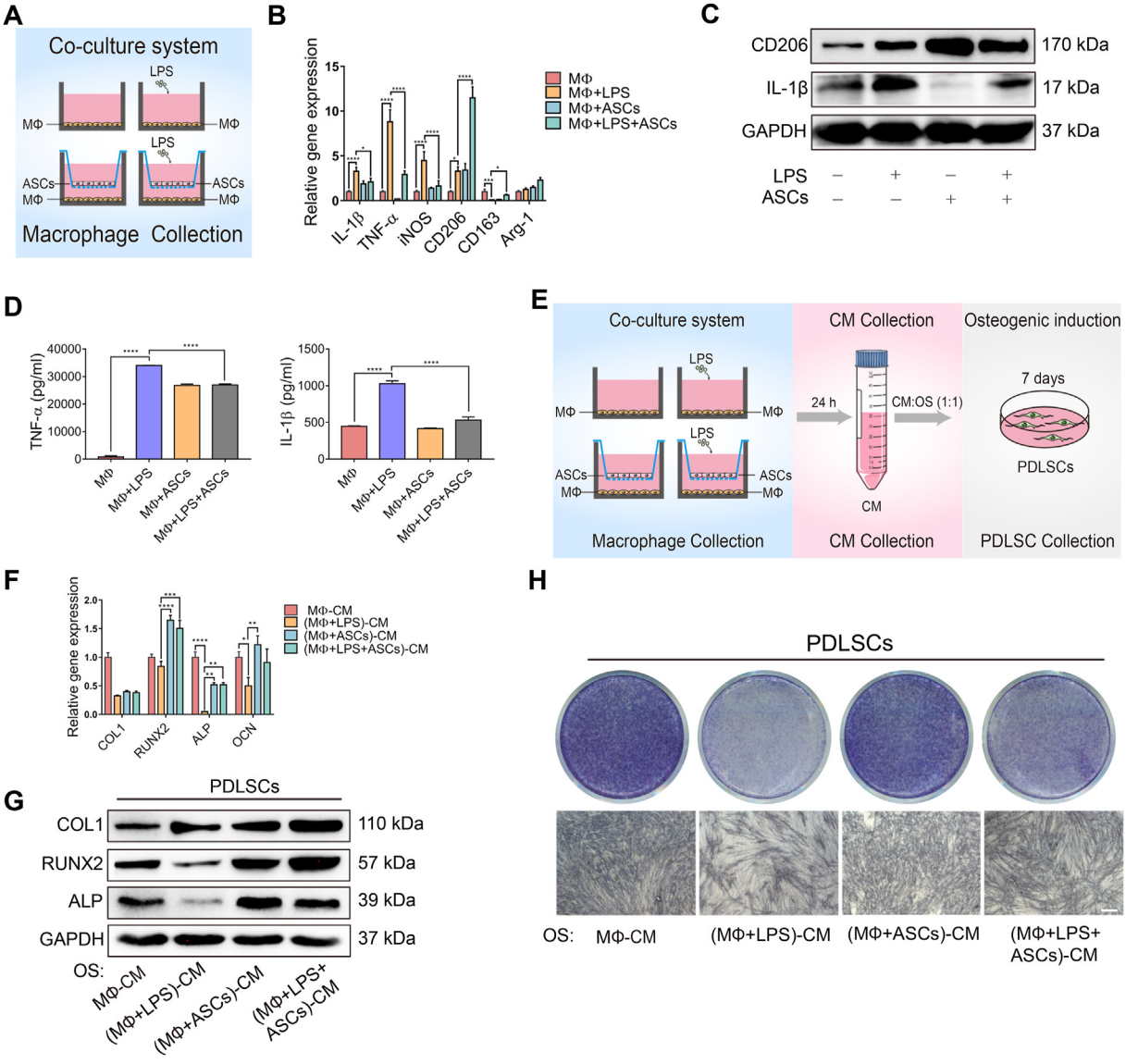

Figure 2: ASCs regulated macrophage polarization and rescued the osteogenic capacity of PDLSCs. (A) Schematic diagram showed the establishment of the ASC-macrophage coculture systems. (B, C) The mRNA expression and the protein levels of M1 markers and M2 markers were measured by RT-qPCR and western blotting. (D) ELISA analysis of the release of the inflammatory cytokines TNF-α and IL-1β in the different groups. (E) Schematic diagram displayed the CM to induce PDLSC osteogenesis. (F, G) The osteogenic markers were measured in PDLSCs at the mRNA and protein levels. (H) ALP staining of the PDLSCs in different CM. Scale bar, 100 μm. CM, conditioned medium.

related transcription factor-2 (RUNX2) (1:1000, 12556, CST, MA, USA), ALP (1:1000, ab67228, Abcam), NRF2 (1:1000, ab62352, Abcam), NAD(P)H quinone oxidoreductase 1 (NQO1) (1:10,000, ab80588, Abcam), CD206 (1:1000, ab125028, Abcam), iNOS (1:1000, 18985-1-AP, Proteintech, Wuhan, China), IDO (1:1000, ab211017, Abcam), IL-1β (1:1000, A1112, Abclonal), AhR (1:1000, ab190797, Abcam), PCNA (1:500, bs-0754R, Bioss), GAPDH (1:2000, Bioss) were used. The secondary antibody goat anti-rabbit IgG H&L (HRP) (1:5000, ab205718, Abcam) was used. The images were detected by using ChemiDocTM MP Imaging System (Bio-Rad, USA).

2.15. Detection of oxidative stress

The reactive oxygen species (ROS) levels in macrophages were detected by ROS Assay Kit (Beyotime). After LPS stimulation or cocultured with ASCs for 12 h, cells were incubated with 1 mL of 0.1% dichlorofluorescin diacetate (DCFH-DA, Biosharp, Hefei, China) at 37 °C for 30 min and were washed with RPMI 1640 medium (Sigma—Aldrich). Then fluorescence microscope was used to evaluate the green fluorescence.

2.16. Transfections with siRNA

Human siRNA-Nrf2 and siRNA-NC (Sangon, Shanghai, China) and Lipofectamine 3000 (Thermo Fisher, MA, USA) were used to transfect macrophages (5×10^5) according to the manufacturer's instructions. After 24 h, cells were dealt with indicated stimulations. RT-qPCR and western blotting were performed to examine the transfection efficiency.

2.17. Chromatin immunoprecipitation (ChIP)-qPCR

Chromatin immunoprecipitation kit were applied to immunoprecipitate chromatin from macrophages referred to the manufacturer's instructions. The majority of the sheared DNA was 200 bp in length, which was detected by ethidium bromide gel electrophoresis. Rabbit

anti-AhR (83200, CST) was used to immunoprecipitate the purified chromatin and then RT-qPCR was performed to detect the amount of specific DNA sequence. The primer set 1: F:5′-GTTTGCCTTTGACGACCTG-3'; R:5′-GCCCTCCTCTGAACTCCC-3′. The primer set 2: F:5′ CCCAAATAGTAGCGAGGAGAG 3′; R:5′-TGGAG-GAGCAAGAAAGAACA-3′.

2.18. Multiple reaction monitoring (MRM)-based targeted metabolomic analysis

Supernatant from ASC cultures was obtained to measure the metabolites of tryptophan. Each sample was pipetted 1.4 mL to dry with nitrogen and was added 0.5 mL acetonitrile-methanol—water (2:2:1, v/v/v) and 10 μL (2 μg/mL) internal standard solution respectively. Then they were mixed by a vortex for 30 s, 4 °C conditions. After being centrifuged under 14,000*g* for 15 min, the supernatant was collected and passed through the HLB plate. The supernatant was then injected for high-performance liquid chromatography mass spectrometry (HPLC-MS/MS) analysis.

Briefly, the separation was performed on a UPLC system (Agilent 1290 Infinity UHPLC) on a C-18 column (Waters, CSH C18 1.7 μm, 2.1 mm × 100 mm column) by gradient elution. QTRAPTM 5500 (AB SCIEX) was performed in positive ion modes. MRM method was used for mass spectrometry quantitative data acquisition. MultiQuant or Analyst was used for quantitative data processing.

2.19. Statistical analysis

Statistical analyses were conducted by GraphPad Prism 7.0 (GraphPad Software, USA). Data were presented as the mean ± SEM. Statistical significance was evaluated by two samples t-test or one-way ANOVA with Tukey's post hoc test for multigroup comparisons, and the level of significance was considered as P values < 0.05.

3. RESULTS

3.1. ASCs reduced alveolar bone loss and regulated macrophage polarization in experimental periodontitis

ASCs and PDLSCs were isolated, and their stemness was verified (Supplementary Figs. 1A—D). After establishing experimental rat models of periodontitis using ligatures for 21 days, ASCs or PBS were injected into the palatal side of the rat maxillary second molar (Figure 1A, B). ASC administration significantly reduced alveolar bone loss compared with the PBS groups, as determined by Micro-CT (Figure 1C). The loss of height of the alveolar bone (CEJ-ABC distance) was diminished after a 21-day ASC injection. Moreover, bone mass parameters were significantly improved with increased BV/TV and Tb. Th and decreased Tb. Sp on day 7 (Figure 1D).

Classically, macrophages are endowed with functional plasticity in response to environmental stimuli, shifting from M1 (pro-inflammatory) to M2 (anti-inflammatory) phenotypes. Despite the small proportional distribution (less than 5—7%) of the inflammatory cell population in periodontitis lesions, macrophages exhibit essential roles in the progression and healing of periodontitis [25], yet little is known about ASC regulation of macrophages in periodontitis. Immunofluorescence staining was performed to analyze the distribution of M1 and M2 macrophages after ASC injection. The ratio of M1-like macrophages ($iNOS^+$)/M2-like macrophages ($CD206^+$) was dramatically decreased in ASC-infused groups compared with PBS groups (Figure 1E, F), suggesting that macrophage polarization played a pivotal role in ASC therapeutic effects in experimental periodontitis. Moreover, ASCs also suppressed the expression of inflammatory factor (IL-1β) from day 7 to day 21 and enhanced that of the osteogenic protein (OCN) from day 14 to day 21 in periodontal tissues, as determined by immunohistochemical staining (Supplementary Fig. 2A—C).

3.2. ASCs regulated macrophages to rescue the osteogenic ability of PDLSCs in inflammatory conditions

To further explore ASC regulation on macrophages *in vitro*, macrophages were cocultured with ASCs (Figure 2A). ASCs significantly promoted the mRNA expression of M2 macrophage markers (CD206, CD163) while diminished M1 macrophage markers (TNF-α, IL-1β, iNOS) compared with macrophages cultured alone with LPS stimulation (Figure 2B), which was further confirmed by immunofluorescence staining (Supplementary Fig. 3). Similarly, ASCs significantly upregulated the protein levels of CD206 while downregulated the expression of IL-1β in macrophages (Figure 2C). Meanwhile, ELISA revealed that the secretion of inflammatory cytokines (TNF-α, IL-1β) was suppressed (Figure 2D).

Considering PDLSCs are crucial for periodontal tissue repair and regeneration in periodontitis, the CM of the cocultured cells was subsequently collected to examine the osteogenic capacity of PDLSCs (Figure 2E). Interestingly, CM of LPS-stimulated macrophages notably limited the osteogenic ability of PDLSCs, with mRNA and protein levels of the osteogenic markers RUNX2, ALP, and OCN significantly downregulated (Figure 2F, G). In contrast, CM of ASCs cocultured with macrophages reversed this effect, although there was no significant difference in the mRNA expression of COL1 (Figure 2F, G). Likewise, CM of ASCs cocultured with macrophages also rescued ALP activity in PDLSCs compared with CM of macrophages in inflammatory conditions (Figure 2H). Hence, these results suggested that ASCs protected PDLSC osteogenic capacity by shifting macrophages into M2 phenotypes and suppressing inflammation.

Additionally, to test the direct effect of ASCs on the osteogenic capacity of PDLSCs in inflammatory conditions, CM of ASCs was applied to culture PDLSCs with osteogenic induction and 1 μg/mL LPS stimulation for 7 days or 21 days. As indicated by RT-qPCR and western blotting, ASCs exerted minor effects on the osteogenic capacity of PDLSCs (Supplementary Fig. 4A and B). ALP staining for 7 days and ARS staining for 21 days exhibited no significant difference (Supplementary Fig. 4C).

3.3. ASCs regulated macrophages through NRF2 activation

The macrophage inflammatory response leads to the production of a large amount of ROS. At the same time, ROS, as a signaling molecule, participates in regulating the polarization of M1/M2 macrophages [26]. Considering the inflammatory response of macrophages is closely related to oxidative stress, ROS levels were determined in macrophages cocultured with ASCs with or without LPS stimulation. As expected, ASCs significantly down-regulated ROS levels of LPS-stimulated macrophages (Supplementary Fig. 5A). Next, we screened several antioxidant genes in the macrophages and observed that the expression of NRF2 and its downstream gene NQO1 were both significantly increased when macrophages were cocultured with ASCs (Supplementary Fig. 5B). Similarly, the protein levels of NRF2 and NQO1 were enhanced by ASCs (Supplementary Fig. 5C). The activation of NRF2 by ASCs was further confirmed by upregulation of nucleoprotein expression and nuclear translocation (Supplementary Fig. 5D and E).

Moreover, immunohistochemical staining uncovered that NRF2 expression was increased on day 7 and peaked on day 14 in ASC-infused groups (Figure 3A). M2-like macrophages ($CD206^+$ green) expressed higher levels of NRF2 (red) in ASC-treated rats compared with those in the PBS groups (Figure 3B), indicating that ASCs could promote NRF2 expression to regulate macrophage polarization.

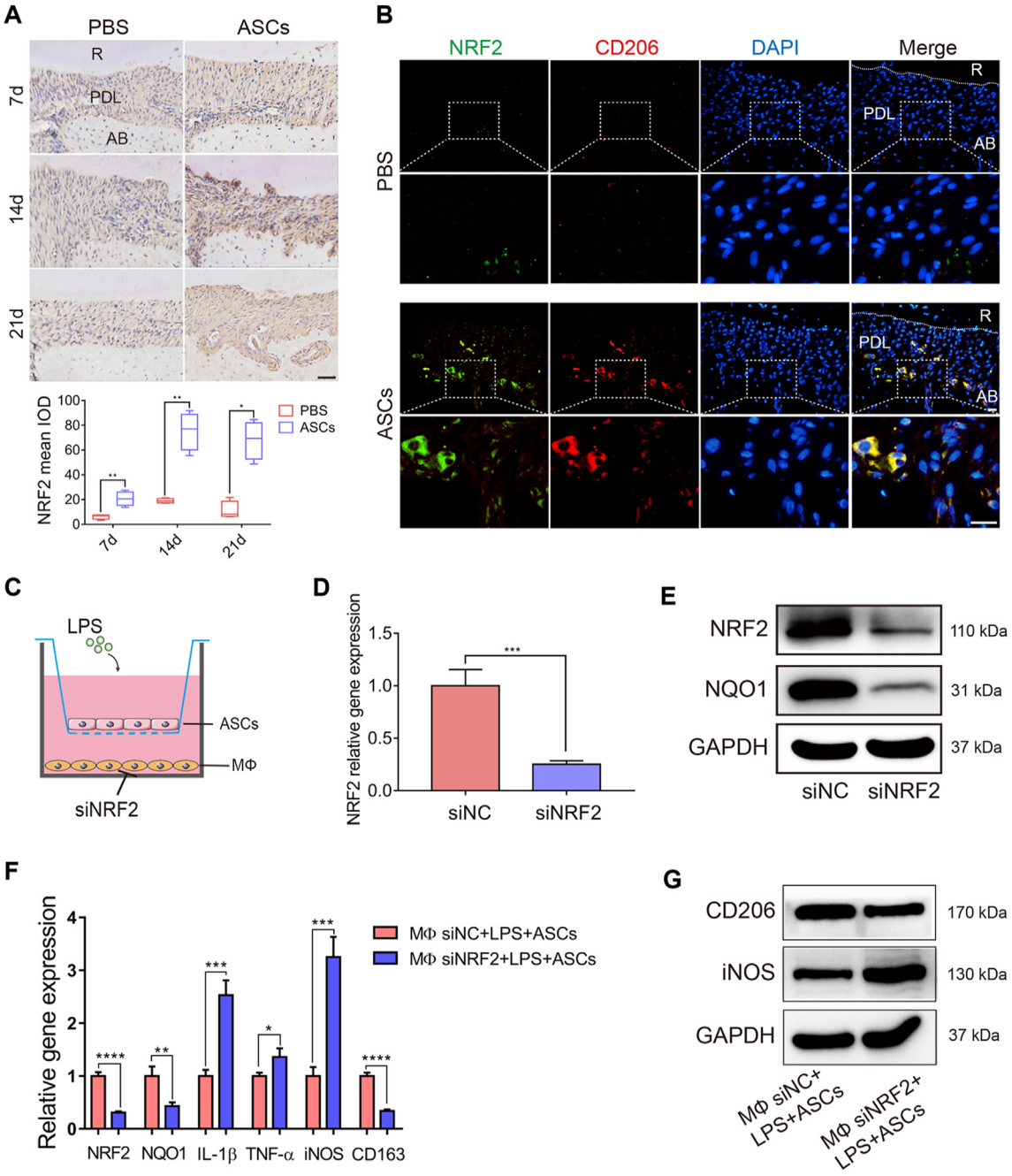

Figure 3: ASCs modulated macrophage polarization through NRF2. (A) Representative immunohistochemical staining of NRF2 in the PBS-injected and ASC-injected rats on day 7, day 14, and day 21. Scale bar, 50 μm. (B) Representative immunofluorescence staining of NRF2 (Green) and M2 macrophages ($CD206^{+}$; Red) in sagittal sections of maxillary molars in PBS-injected and ASC-injected rats. Scale bar, 20 μm. (C) Schematic diagram of knocking down NRF2 in macrophages and macrophages cocultured with ASCs and LPS stimulation. (D, E) RT-qPCR and western blotting were used to measure the NRF2 siRNA or siNC in macrophages. (F, G) The mRNA expression and protein levels of M1 markers were increased, while those of M2 markers were decreased after silencing NRF2 in the cocultured groups. R, root; PDL, periodontal ligament; AB, alveolar bone; siRNA, small interfering RNA; NC, negative control. All data were expressed as mean ± SD; *P < 0.05, **P < 0.01, ***P < 0.001.

Earlier studies have established that besides regulating oxidative stress homeostasis, NRF2 mediated macrophage polarization [27,28]. To further confirm its role in the ASC regulation of macrophages, NRF2 was knocked down in macrophages (Figure 3C–E). Interestingly, knocking down NRF2 reversed ASC regulation on macrophages. The mRNA expression or the protein levels of M1 markers (TNF-α, IL-1β, and iNOS) were substantially upregulated, whereas those of the M2 markers (CD206 and CD163) were decreased (Figure 3F, G). Collectively, these results demonstrated that ASCs promoted NRF2 activation in macrophages, thereby mediating ASC regulation on macrophages.

3.4. IDO activity mediated ASC modulation on macrophages and the subsequent protection of PDLSC osteogenesis

Previous studies showed that several factors mediated ASC immunomodulatory capacities, including the regulation of macrophages [29]. To investigate the factors that mediated ASC regulation on macrophages, immune-regulatory factors of ASCs were screened. The expression of IDO-1 in ASCs in the presence of LPS was dramatically increased compared with other factors (Figure 4A). Additionally, the protein level of IDO-1 was also highly expressed (Figure 4B). To verify the role of IDO in the modulation of ASCs on macrophages, ASCs were pretreated with an IDO enzymic activity inhibitor, 1-MT, for 24 h (Figure 4C). The results showed that 1-MT treatment significantly reversed ASC regulation on macrophages, with mRNA or protein levels of M1 markers (iNOS, TNF-α, IL-1β) upregulated while those of M2 marker (CD206, CD163) were downregulated (Figure 4D, E). Immunofluorescence staining of IL-1β, iNOS, CD206, and CD163 revealed a similar trend (Supplementary Fig. 6). Moreover, the secretion of inflammatory factors (TNF-α and IL-1β) was increased following 1-MT administration (Figure 4F).

The CM of 1-MT-pretreated ASCs cocultured with macrophages was used to induce PDLSC osteogenesis (Supplementary Fig. 7A). As expected, the osteogenic capacity of PDLSCs was downregulated in the 1-MT treatment groups (Supplementary Fig. 7B—E). Thus, IDO enzymic activity mediated ASC regulation on macrophages and subsequent enhancement of PDLSC osteogenic capacity.

3.5. Kyn derived from ASCs mediated by IDO modulated macrophages through NRF2

Given that IDO is a key enzyme in the metabolic pathway of tryptophan, the main tryptophan metabolites were examined to test whether the tryptophan metabolites participated in the ASC regulation of macrophage (Figure 5A, B). After LPS stimulation, the ratio of Trp/Kyn in the ASC supernatant was reduced, with Trp decreased and Kyn increased (Figure 5C), confirming the increase in IDO activity. To explore whether the increased levels of Kyn secreted by ASCs exerted a similar effect on macrophages, Kyn was added to the macrophages cocultured with 1-MT-pretreated ASCs (Figure 5D). Interestingly, Kyn rescued the impaired modulatory abilities of 1-MT-pretreated ASCs on macrophages, with the mRNA expression of IL-1β, TNF-α and iNOS decreased, whereas that of CD206, CD163, and arginase (Arg)-1 increased (Figure 5E). Besides, the protein level of CD206 was increased while the protein levels of iNOS and IL-1β were decreased when Kyn was adding (Figure 5F). These data suggested that Kyn derived from ASCs, which was catalyzed by IDO, mediated ASC regulation on macrophages.

It is worthwhile pointing out that NRF2 expression was significantly downregulated in the 1-MT pretreatment group, whereas the addition of Kyn enhanced NRF2 expression in macrophages (Supplementary Fig. 8A and B), implying that IDO-mediated Kyn might influence macrophage polarization through NRF2 activation. Therefore, the expression of NRF2 was silenced in macrophages (Supplementary Fig. 8C). As expected, suppressing NRF2 inhibited the effect of Kyn on LPS-macrophages at both mRNA and protein levels (Supplementary Fig. 8D and E). Altogether, these findings reflect that IDO-mediated Kyn derived from ASCs promoted the expression of M2 macrophages and inhibited M1 macrophages in the inflammatory environment through NRF2 activation.

3.6. Inhibition of IDO activity in ASCs reduced the therapeutic effects in experimental periodontitis and downregulated the expression of NRF2

To further investigate the effects of IDO activity in ASCs in experimental periodontitis *in vivo*, 1-MT-pretreated ASCs were injected into periodontitis rats. As demonstrated by Micro-CT, the CEJ-ABC distance, and Tb. Sp were increased in 1-MT groups, albeit only the increase in CEJ-ABC distance on day 21 was significant. Other bone mass parameters such as BV/TV and Tb. Th were significantly decreased, indicating more bone loss in the 1-MT groups (Figure 6A, B).

Furthermore, OCN expression was reduced, and IL-1β expression and the ratio of $iNOS^{+}/CD206^{+}$ were increased when the IDO activity of ASCs was inhibited (Figure 6C—E). Besides, the expression of NRF2 was significantly reduced in the 1-MT pretreatment groups compared with the ASC-injected groups (Figure 6C, E).

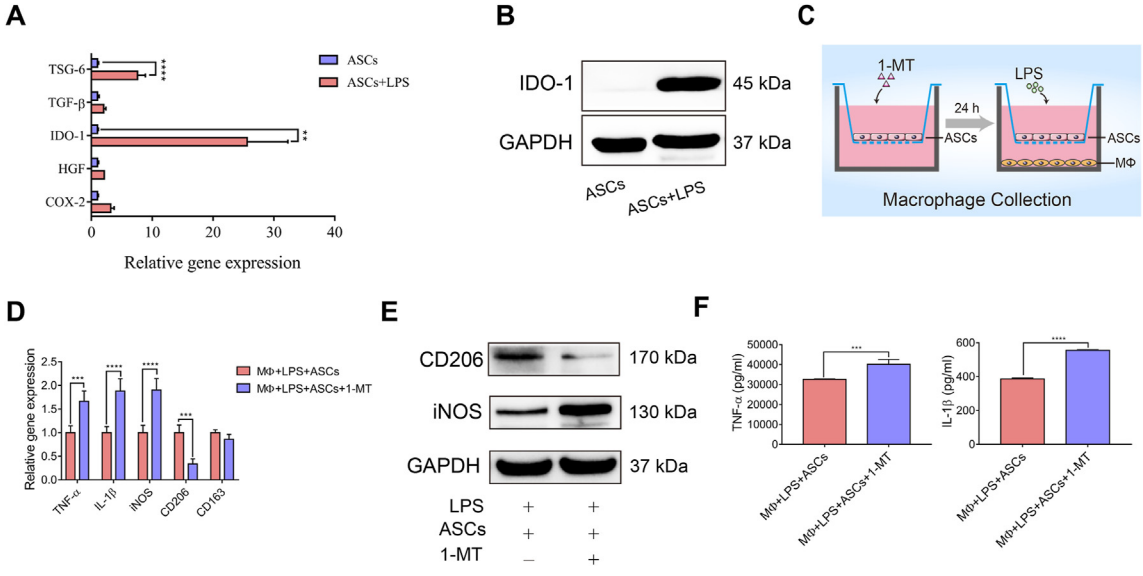

Figure 4: IDO activity mediated ASC modulation on macrophages. (A) The mRNA level of immunoregulatory factors in ASCs and ASCs stimulated with LPS. (B) The protein level of IDO-1 was detected in ASCs and ASCs stimulated with LPS. (C) Schematic diagram of inhibition of IDO-1 activity in ASCs treated with 1-MT in the coculture system. (D, E) The mRNA expression and protein levels of M1 and M2 markers in 1-MT-pretreated ASCs cocultured with macrophages, and ASCs cocultured with macrophages. (F) ELISA analysis of the release of the inflammatory cytokines TNF-α and IL-1β.

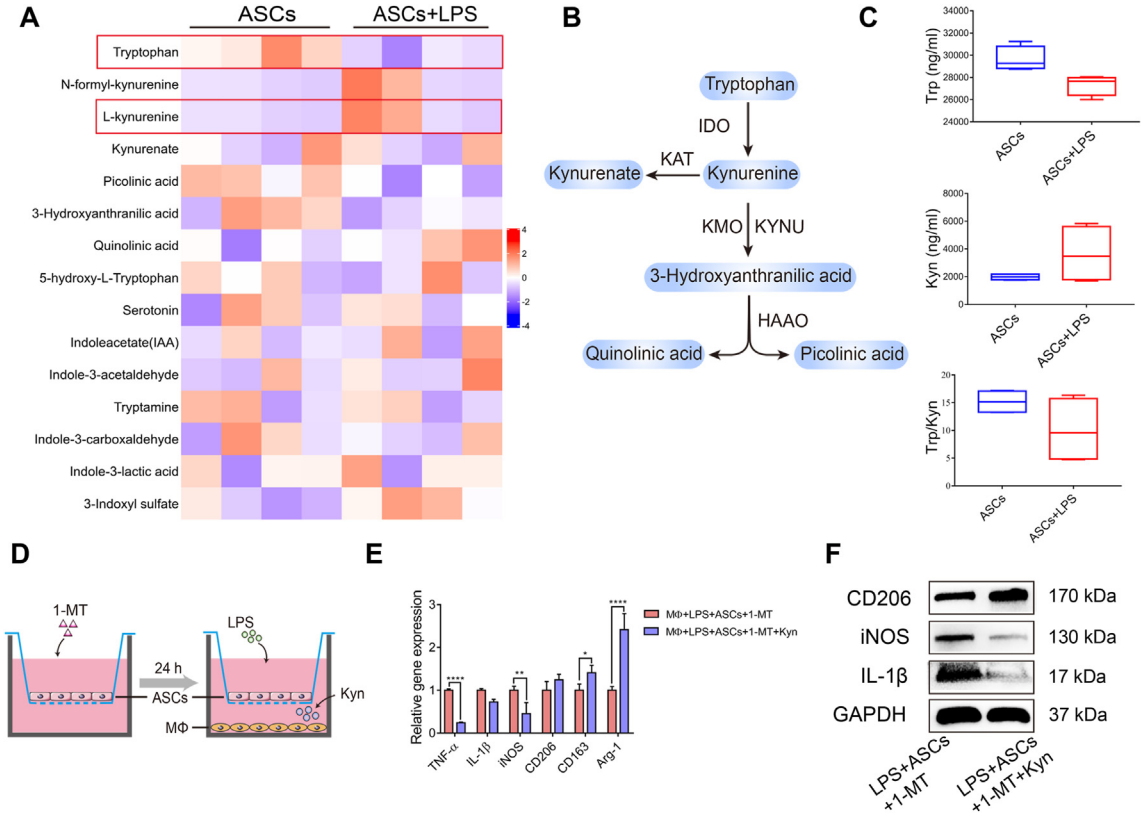

Figure 5: ASC-derived Kyn inhibited the expression of M1 macrophages and promoted that of M2 macrophages. (A) The heatmap of the tryptophan metabolites in the supernatants of ASCs and 24 h LPS-stimulated ASCs. (B) IDO-mediated Trp metabolism along the kynurenine pathway. (C) The concentration of Trp and Kyn and the ratio of Trp/Kyn. (D) The schematic diagram of the addition of 500 μM Kyn in macrophages cocultured with 1-MT-pretreated ASCs. (E, F) The mRNA levels and protein levels of M1 and M2 markers were detected by RT-qPCR and western blotting. Trp, tryptophan; Kyn, kynurenine.

3.7. Kyn activated NRF2 through AhR binding

As previously documented, Kyn served as a potent ligand to AhR, whose activation can further activate NRF2 [30]. To elucidate the underlying mechanism by which Kyn activated NRF2 in macrophages, we first detected the expression of AhR and its downstream targets (Cytochrome P450 (CYP) 1A1 and CYP1B1) and NRF2 following Kyn administration. The results revealed that Kyn promoted both the mRNA and protein levels of AhR and NRF2 (Figure 7A, B). Furthermore, Kyn enhanced the nucleoprotein expression of AhR and NRF2 (Figure 7C, D), which was further confirmed by immunofluorescence staining (Supplementary Fig. 8F and G), indicating the increase of nuclear translocation of AhR and NRF2. Whereas, the specific AhR antagonist CH-223191 (CH, 20 μM) inhibited AhR activation and subsequent NRF2 expression and activation (Figure 7A—D). Finally, the ChIP-qPCR assay demonstrated that AhR could directly bind to the NRF2 promoter, and Kyn significantly enhanced this binding capacity (Figure 7E, F).

4. DISCUSSION

Herein, we discovered that ASCs regulated macrophages to rescue PDLSC osteogenesis through the IDO-mediated Trp-Kyn metabolic pathway in periodontitis. Further investigations uncovered that Kyn derived from ASCs activated AhR and enhanced its binding to NRF2 promoter in macrophages, thereby promoting macrophages toward anti-inflammatory phenotypes (Figure 7G).

Our study demonstrated the therapeutic efficiency of ASC injection in periodontitis via micro-CT analysis, reducing the alveolar bone loss and improving bone density parameters. Moreover, ASCs reduced the inflammatory cytokine expression, diminished the ratio of $iNOS^{+}$/$CD206^{+}$ macrophages, and promoted the expression of the osteogenic protein, which is in line with the findings of E. Mohammed et al. that ASC injection significantly promoted the formation of new tissues in periodontitis rats [31].

IDO, regarded as a potent immune regulator of MSCs, is also a critical initial enzyme of Trp metabolism [32]. In this context, IDO-mediated MSC immunometabolism has attracted much interest in MSC-based therapy research [33—35]. Evidence showed that IDO mediated MSC regulation on macrophages, skewing macrophages towards anti-inflammatory phenotypes [29,36], though the evidence was weak. In our present study, we demonstrated that IDO expression and activity were dramatically upregulated in ASCs when exposed to inflammation. Furthermore, the IDO enzymatic activity inhibitor 1-MT impaired ASC regulation on macrophages. The therapeutic effects of ASCs on rat models of periodontitis were significantly counteracted by 1-MT, with increased alveolar bone loss and inflammatory macrophages.

It was previously reported that IDO catalyzed Trp into several bioactive intermediates, including Kyn, Ka, and 3-hydroxyanthranilic acid (3-Haa), which exerted various effects on immune cells [21,37,38]. However, the molecular mechanism of ASC regulation on macrophages through IDO remained poorly understood. In our study, we found that compared with naïve ASCs, LPS-treated ASCs released more Kyn and fewer Trp, indicating a high IDO metabolic activity, which was consistent with the findings of previous studies [11,39]. Nevertheless, the secretion of other metabolites Ka and 3-Haa did not

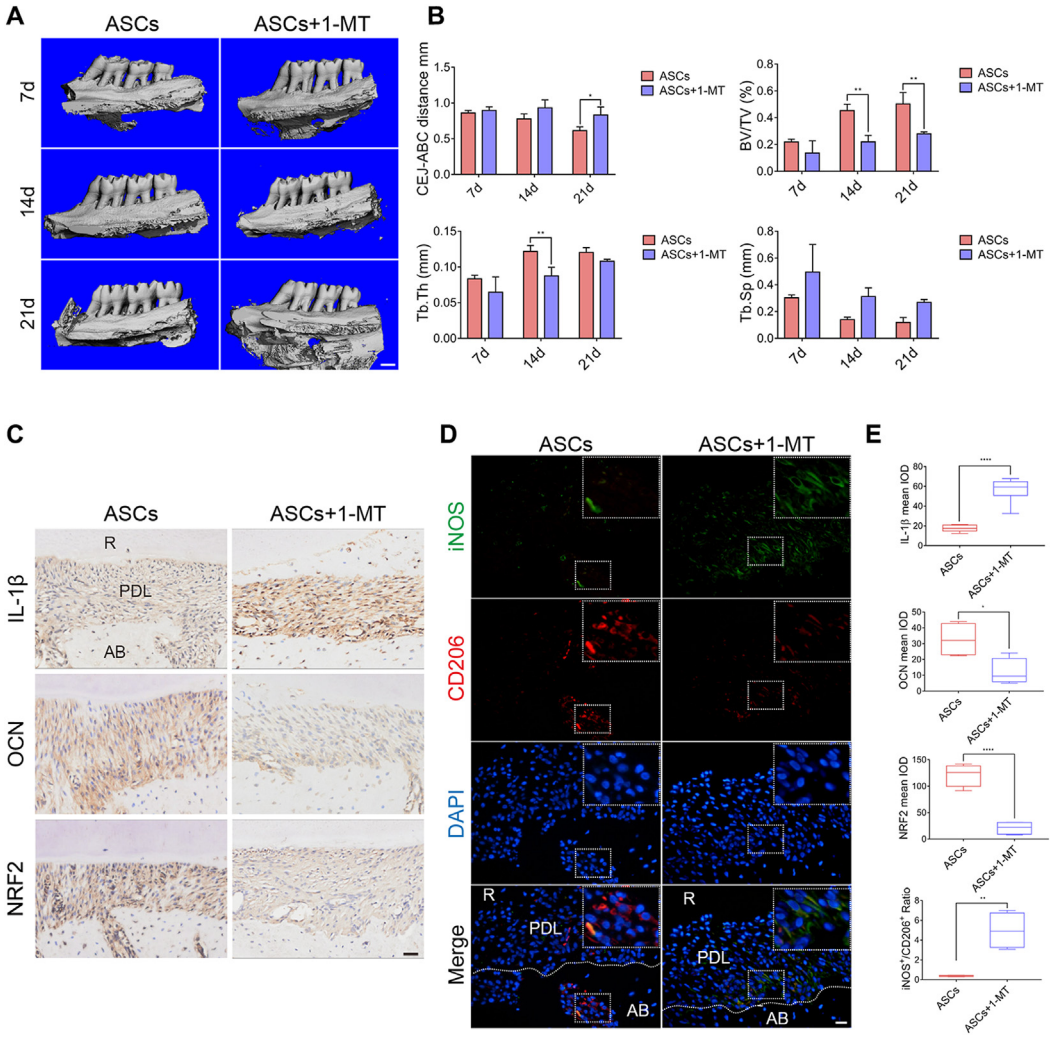

Figure 6: Inhibition of IDO activity reduced the therapeutic potential of ASCs in experimental periodontitis and downregulated NRF2 expression. (A) Three-dimensional reconstruction of maxillary alveolar bone in ASC-injected and 1-MT pretreated ASC-injected rats on day 7, day 14, and day 21. Scale bar, 1 mm. (B) Analysis of bone parameters. (C) Immunohistochemical staining of IL-1β, OCN, and NRF2 in the ASC-injected and 1-MT pretreated ASC-injected rats. Scale bar, 50 μm. (D) Representative immunofluorescence staining of M1 phenotype macrophages ($iNOS^+$; Green) and M2 macrophages ($CD206^+$; Red) in sagittal sections of maxillary molars in ASC-injected and 1-MT pretreated ASC-injected rats. Scale bar, 20 μm. (E) The mean IOD of IL-1β, OCN, and NRF2 and the calculated ratio of $iNOS^+/CD206^+$. IOD, integrated optical density.

increase, suggesting that Kyn could be the primary mediator of ASC immunomodulation. Kyn has been proven to exert immunosuppressive effects on T cells and NK cells [40]. Notably, Campesato et al. demonstrated that Kyn promoted the proliferation of regulatory T cells, thereby promoting the enhancement of M2-like tumor macrophages by binding to AhR [41]. In our study, Kyn suppressed the inflammatory response of LPS-stimulated macrophages and promoted the expression of $CD206^+$ macrophages. Moreover, the impaired regulation of macrophages in 1-MT-treated ASCs was rescued by Kyn supplements. Taken together, our results established that metabolite Kyn of ASCs mediated the regulation of macrophages.

Interestingly, we discovered that ASCs promoted NRF2 expression and activation in macrophages. Prior studies have shown that NRF2 exerted anti-inflammatory effects in macrophages. Activation of NRF2 through the alkylation of KEAP1 via the endogenous metabolite itaconate suppressed the pro-inflammation (IL-1β and IFN-β) in macrophages [42]. Therefore, we inferred that ASCs modulated macrophages through NRF2 activation. Moreover, our study found that ASCs enhanced the simultaneous expression of NRF2 and CD206 in rat models of periodontitis, while silencing NRF2 in macrophages *in vitro* diminished the effect of ASCs on macrophages. 1-MT-treated ASCs failed to induce NRF2 expression in macrophages, while Kyn reversed this effect. Given that Kyn served as a potent ligand of AhR that can further regulate the gene transcription of NRF2 [41,43], an interaction between Kyn, AhR, and NRF2 in macrophage regulation was expected. In our study, Kyn induced AhR and NRF2 activation, whereas the use of the AhR-specific inhibitor CH blocked NRF2 expression and activation. Furthermore, we discovered that Kyn enhanced AhR binding to the NRF2 promoter. Taken together, Kyn mediated macrophage regulation by activating AhR, directly promoting NRF2 expression.

PDLSCs are regarded as the main functional cells for periodontal tissue repair and regeneration, which are influenced by macrophage polarization. However, in periodontitis, the osteogenic capacity of PDLSCs was severely impaired due to inflammatory cytokines [44]. Prior studies

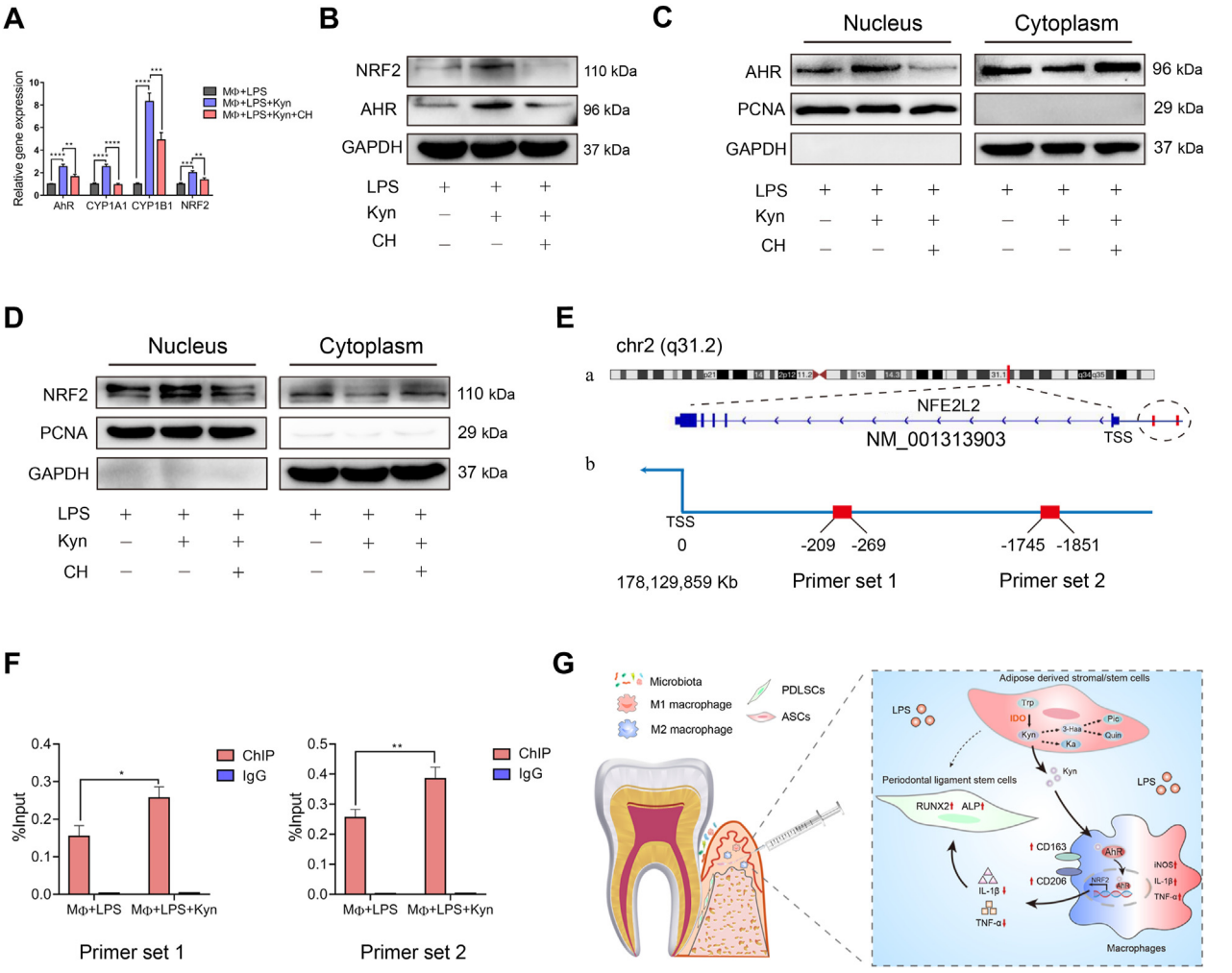

Figure 7: Kyn activated NRF2 through AhR signaling. (A) Macrophages were pretreated with CH-223191 (CH, 20 μM) for 2 h before the addition of Kyn to the culture for 24 h. The mRNA levels of AhR, CYP1A1, CYP1B1, and NRF2 were measured by RT-qPCR. (B) The total protein levels of NRF2 and AhR were detected by western blotting. (C) The nuclear and cytoplasmic protein levels of AhR in macrophages were detected by western blotting. (D) The nuclear and cytoplasmic protein levels of NRF2 in macrophages were detected by western blotting. (E) (a) The location of the gene sequence of NFE2L2 (also known as NRF2) on chromosome 2. (b) The locations of the binding sites were upstream of the TSS. (F) ChIP-qPCR analysis of the interaction between AhR and the NRF2 promoter. (G) A schematic overview of IDO-mediated ASC regulation on macrophages in periodontitis. TSS, transcription start site; IDO, indoleamine 2,3-dioxygenase; ASC, adipose-derived stromal/stem cells.

showed that the CM of M2 macrophages promoted PDLSC osteogenic and cementoblastic differentiation through Akt and JNK signaling [45], while the CM of M1 macrophages impaired osteogenesis [46]. Consistently, we found that the secretion of the inflammatory cytokines TNF-α and IL-1β in macrophages were significantly reduced by ASCs, which could explain the recovery of PDLSC osteogenesis. However, in our study, the direct effects of ASCs on PDLSC osteogenesis in the inflammatory environment were minor, which implied the indirect influence of ASCs on PDLSCs in periodontal tissue regeneration.

In fact, besides macrophages, other immune cells, especially T cells, also play a critical role in periodontal regeneration. Considering the potent IDO-mediated immunomodulation of MSCs on T cells [34], further evidence with regard to T cells regulated by ASCs in periodontitis, as well as the underlying mechanism, is required.

Taken together, ASCs exhibited effective therapeutic potentials in experimental periodontitis. This mechanistic study provided promising approaches such as activators or gene manipulation to activate the IDO pathway in ASCs, to enhance ASC immunomodulation and therapeutic efficiency in periodontitis.

5. CONCLUSION

In summary, we demonstrated the therapeutic effects of ASCs in experimental periodontitis and uncovered a metabolic mechanism by which ASCs modulate macrophages, which provided a scientific basis for potential strategies of manipulating tryptophan metabolism to enhance ASC-based therapeutic efficiency in periodontitis.

AUTHOR CONTRIBUTION

Hanyue Li: Data curation, Formal analysis, Software, Validation, Writing-original draft. Yuan Yu: Formal analysis, Investigation. Hongying Chen: Methodology, Resources. Hongwei Dai: Conceptualization,

Funding acquisition, Writing-review & editing. Jie Li: Conceptualization, Funding acquisition, Project administration.

AVAILABILITY OF DATA AND MATERIAL

All data generated or analyzed using this study was included in the article and Supplementary materials.

DATA AVAILABILITY

Data will be made available on request.

ACKNOWLEDGEMENT

This study was supported by National Natural Science Foundation of China (No. 82071072), Scientific and Technological Research Program of Chongqing Municipal Education Commission (No. KJQN202000417) and Natural Science Foundation of Chongqing Yuzhong District (No. 20200113).

DECLARATION OF COMPETING INTERESTS

The authors declare that they have no known competing financial interests or personal relationships that could have appeared to influence the work reported in this paper.

APPENDIX A. SUPPLEMENTARY DATA

Supplementary data to this article can be found online at https://doi.org/10.1016/j.molmet.2022.101617.

REFERENCES

[1] Tobita, M., Mizuno, H., 2010. Periodontal disease and periodontal tissue regeneration. Curr Stem Cell Res Ther 5:168—174.
[2] Yoshida, T., Washio, K., Iwata, T., Okano, T., Ishikawa, I., 2012. Current status and future development of cell transplantation therapy for periodontal tissue regeneration. Int J Dent 2012:307024.
[3] Li, Q., Yang, G., Li, J., Ding, M., Zhou, N., Dong, H., et al., 2020. Stem cell therapies for periodontal tissue regeneration: a network meta-analysis of preclinical studies. Stem Cell Res Ther 11:427.
[4] Wang, M., Xie, J., Wang, C., Zhong, D., Xie, L., Fang, H., 2020. Immunomodulatory properties of stem cells in periodontitis: current status and future prospective. Stem Cells Int 2020:9836518.
[5] Behdin, S., Alqahtani, H.M., Bissada, N.F., 2020. Therapeutic potential of adipose tissue stem cells for periodontal regeneration. J Periodontol 91:732—733.
[6] Mazini, L., Rochette, L., Amine, M., Malka, G., 2019. Regenerative capacity of adipose derived stem cells (ADSCs), comparison with mesenchymal stem cells (MSCs). Int J Mol Sci 20.
[7] Melief, S.M., Zwaginga, J.J., Fibbe, W.E., Roelofs, H., 2013. Adipose tissue-derived multipotent stromal cells have a higher immunomodulatory capacity than their bone marrow-derived counterparts. Stem Cells Transl Med 2:455—463.
[8] Zhou, W., Lin, J., Zhao, K., Jin, K., He, Q., Hu, Y., et al., 2019. Single-cell profiles and clinically useful properties of human mesenchymal stem cells of adipose and bone marrow origin. Am J Sports Med 47:1722—1733.
[9] Wu, P.H., Chung, H.Y., Wang, J.H., Shih, J.C., Kuo, M.Y., Chang, P.C., et al., 2016. Amniotic membrane and adipose-derived stem cell co-culture system enhances bone regeneration in a rat periodontal defect model. J Formosan Med Assoc Taiwan yi zhi 115:186—194.
[10] Tobita, M., Uysal, C.A., Guo, X., Hyakusoku, H., Mizuno, H., 2013. Periodontal tissue regeneration by combined implantation of adipose tissue-derived stem cells and platelet-rich plasma in a canine model. Cytotherapy 15:1517—1526.
[11] Shi, Y., Wang, Y., Li, Q., Liu, K., Hou, J., Shao, C., et al., 2018. Immunoregulatory mechanisms of mesenchymal stem and stromal cells in inflammatory diseases. Nature Rev Nephrol 14:493—507.
[12] Deng, S., Zhou, X., Ge, Z., Song, Y., Wang, H., Liu, X., et al., 2019. Exosomes from adipose-derived mesenchymal stem cells ameliorate cardiac damage after myocardial infarction by activating S1P/SK1/S1PR1 signaling and promoting macrophage M2 polarization. The Int J Biochem Cell Biol 114:105564.
[13] Kawata, Y., Tsuchiya, A., Seino, S., Watanabe, Y., Kojima, Y., Ikarashi, S., et al., 2019. Early injection of human adipose tissue-derived mesenchymal stem cell after inflammation ameliorates dextran sulfate sodium-induced colitis in mice through the induction of M2 macrophages and regulatory T cells. Cell Tissue Res 376:257—271.
[14] Shen, K., Jia, Y., Wang, X., Zhang, J., Liu, K., Wang, J., et al., 2021. Exosomes from adipose-derived stem cells alleviate the inflammation and oxidative stress via regulating Nrf2/HO-1 axis in macrophages. Free Radical Biol Med 165:54—66.
[15] Garaicoa-Pazmino, C., Fretwurst, T., Squarize, C.H., Berglundh, T., Giannobile, W.V., Larsson, L., et al., 2019. Characterization of macrophage polarization in periodontal disease. J Clin Periodontol 46:830—839.
[16] Li, H., Dai, H., Li, J., 2022. Immunomodulatory properties of mesenchymal stromal/stem cells: the link with metabolism. J Adv Res. https://doi.org/10.1016/j.jare.2022.05.012. In press. https://www.sciencedirect.com/science/article/pii/S2090123222001254.
[17] Wang, G., Cao, K., Liu, K., Xue, Y., Roberts, A.I., Li, F., et al., 2018. Kynurenic acid, an Ido metabolite, controls TSG-6-mediated immunosuppression of human mesenchymal stem cells. Cell Death Differen 25:1209—1223.
[18] Burnham, A.J., Foppiani, E.M., Horwitz, E.M., 2020. Key metabolic pathways in MSC-mediated immunomodulation: implications for the prophylaxis and treatment of graft versus host disease. Front Immunol 11:609277.
[19] Ning, K., Liu, S., Yang, B., Wang, R., Man, G., Wang, D.E., et al., 2022. Update on the effects of energy metabolism in bone marrow mesenchymal stem cells differentiation. Mol Metab 58:101450.
[20] de Castro, L.L., Lopes-Pacheco, M., Weiss, D.J., Cruz, F.F., Rocco, P.R.M., 2019. Current understanding of the immunosuppressive properties of mesenchymal stromal cells. J Mol Med 97:605—618.
[21] Berg, M., Polyzos, K.A., Agardh, H., Baumgartner, R., Forteza, M.J., Kareinen, I., et al., 2020. 3-Hydroxyanthralinic acid metabolism controls the hepatic SREBP/lipoprotein axis, inhibits inflammasome activation in macrophages, and decreases atherosclerosis in Ldlr-/- mice. Cardiovasc Res 116:1948—1957.
[22] Dabrowski, W., Kocki, T., Pilat, J., Parada-Turska, J., Malbrain, M.L., 2014. Changes in plasma kynurenic acid concentration in septic shock patients undergoing continuous veno-venous haemofiltration. Inflammation 37:223—234.
[23] Wirthgen, E., Hoeflich, A., Rebl, A., Gunther, J., 2017. Kynurenic acid: the janus-faced role of an immunomodulatory tryptophan metabolite and its link to pathological conditions. Front Immunol 8:1957.
[24] Li, J., Curley, J.L., Floyd, Z.E., Wu, X., Halvorsen, Y.D.C., Gimble, J.M., 2018. Isolation of human adipose-derived stem cells from lipoaspirates. Method Mol Biol 1773:155—165.
[25] Thorbert-Mros, S., Larsson, L., Berglundh, T., 2015. Cellular composition of long-standing gingivitis and periodontitis lesions. J Periodon Res 50:535—543.
[26] Rendra, E., Riabov, V., Mossel, D.M., Sevastyanova, T., Harmsen, M.C., Kzhyshkowska, J., 2019. Reactive oxygen species (ROS) in macrophage activation and function in diabetes. Immunobiology 224:242—253.
[27] Feng, R., Morine, Y., Ikemoto, T., Imura, S., Iwahashi, S., Saito, Y., et al., 2018. Nrf2 activation drive macrophages polarization and cancer cell epithelial-mesenchymal transition during interaction. Cell Commun Signal: CCS 16:54.

[28] Kobayashi, E.H., Suzuki, T., Funayama, R., Nagashima, T., Hayashi, M., Sekine, H., et al., 2016. Nrf2 suppresses macrophage inflammatory response by blocking proinflammatory cytokine transcription. Nature Communications 7:11624.

[29] Joo, H., Oh, M.K., Kang, J.Y., Park, H.S., Chae, D.H., Kim, J., et al., 2021. Extracellular vesicles from thapsigargin-treated mesenchymal stem cells ameliorated experimental colitis via enhanced immunomodulatory properties. Biomedicines 9.

[30] Singh, R., Chandrashekharappa, S., Bodduluri, S.R., Baby, B.V., Hegde, B., Kotla, N.G., et al., 2019. Enhancement of the gut barrier integrity by a microbial metabolite through the Nrf2 pathway. Nature Commun 10:89.

[31] Mohammed, E., Khalil, E., Sabry, D., 2018. Effect of adipose-derived stem cells and their exo as adjunctive therapy to nonsurgical periodontal treatment: a histologic and histomorphometric study in rats. Biomolecules 8.

[32] Platten, M., Nollen, E.A.A., Rohrig, U.F., Fallarino, F., Opitz, C.A., 2019. Tryptophan metabolism as a common therapeutic target in cancer, neurodegeneration and beyond. Nature Rev Drug Discov 18:379—401.

[33] Zheng, G., Qiu, G., Ge, M., He, J., Huang, L., Chen, P., et al., 2017. Human adipose-derived mesenchymal stem cells alleviate obliterative bronchiolitis in a murine model via Ido. Respir Res 18:119.

[34] Milosavljevic, N., Gazdic, M., Simovic Markovic, B., Arsenijevic, A., Nurkovic, J., Dolicanin, Z., et al., 2018. Mesenchymal stem cells attenuate liver fibrosis by suppressing Th17 cells - an experimental study. Transplant Int Off J Eur Soc Organ Transplant 31:102—115.

[35] Gazdic, M., Simovic Markovic, B., Vucicevic, L., Nikolic, T., Djonov, V., Arsenijevic, N., et al., 2018. Mesenchymal stem cells protect from acute liver injury by attenuating hepatotoxicity of liver natural killer T cells in an inducible nitric oxide synthase- and indoleamine 2,3-dioxygenase-dependent manner. J Tissue Eng Regen Med 12:e1173—e1185.

[36] Francois, M., Romieu-Mourez, R., Li, M., Galipeau, J., 2012. Human MSC suppression correlates with cytokine induction of indoleamine 2,3-dioxygenase and bystander M2 macrophage differentiation. Mol Ther J Am So Gene Ther 20:187—195.

[37] Zang, X., Zheng, X., Hou, Y., Hu, M., Wang, H., Bao, X., et al., 2018. Regulation of proinflammatory monocyte activation by the kynurenine-AhR axis underlies immunometabolic control of depressive behavior in mice. FASEB J Off Pub Feder Am Soc Exp Biol 32:1944—1956.

[38] Lee, T., Park, H.S., Jeong, J.H., Jung, T.W., 2019. Kynurenic acid attenuates pro-inflammatory reactions in lipopolysaccharide-stimulated endothelial cells through the PPARdelta/HO-1-dependent pathway. Mol Cell Endocrinol 495:110510.

[39] de Witte, S.F.H., Merino, A.M., Franquesa, M., Strini, T., van Zoggel, J.A.A., Korevaar, S.S., et al., 2017. Cytokine treatment optimises the immunotherapeutic effects of umbilical cord-derived MSC for treatment of inflammatory liver disease. Stem Cell Res Ther 8:140.

[40] Trikha, P., Moseman, J.E., Thakkar, A., Campbell, A.R., Elmas, E., Foltz, J.A., et al., 2021. Defining the AHR-regulated transcriptome in NK cells reveals gene expression programs relevant to development and function. Blood Adv 5: 4605—4618.

[41] Campesato, L.F., Budhu, S., Tchaicha, J., Weng, C.H., Gigoux, M., Cohen, I.J., et al., 2020. Blockade of the AHR restricts a Treg-macrophage suppressive axis induced by L-Kynurenine. Nature Commun 11:4011.

[42] Mills, E.L., Ryan, D.G., Prag, H.A., Dikovskaya, D., Menon, D., Zaslona, Z., et al., 2018. Itaconate is an anti-inflammatory metabolite that activates Nrf2 via alkylation of KEAP1. Nature 556:113—117.

[43] Miao, W., Hu, L., Scrivens, P.J., Batist, G., 2005. Transcriptional regulation of NF-E2 p45-related factor (NRF2) expression by the aryl hydrocarbon receptor-xenobiotic response element signaling pathway: direct cross-talk between phase I and II drug-metabolizing enzymes. J Biol Chem 280: 20340—20348.

[44] Cao, Y., Wang, Y., Li, C., Jiang, Q., Zhu, L., 2021. Effect of TNF-alpha on the proliferation and osteogenesis of human periodontal mesenchymal stem cells. Exp Therap Med 21:434.

[45] Li, X., He, X.T., Kong, D.Q., Xu, X.Y., Wu, R.X., Sun, L.J., et al., 2019. M2 macrophages enhance the cementoblastic differentiation of periodontal ligament stem cells via the Akt and JNK pathways. Stem Cell 37:1567—1580.

[46] He, X.T., Li, X., Yin, Y., Wu, R.X., Xu, X.Y., Chen, F.M., 2018. The effects of conditioned media generated by polarized macrophages on the cellular behaviours of bone marrow mesenchymal stem cells. J Cell Mol Med 22: 1302—1315.

